ARTICLE   OPEN

Check for updates

Evaluation of polyvinyl chloride adhesion to 2D crystal flakes

Yusai Wakafuji[1], Momoko Onodera[1 ✉], Satoru Masubuchi [1], Rai Moriya [1], Yijin Zhang[1], Kenji Watanabe [2], Takashi Taniguchi [1,3] and Tomoki Machida [1 ✉]

We investigated the adhesion of polyvinyl chloride (PVC) to 2D crystal flakes on SiO$_2$/Si substrates. Although the anchoring effect cannot be used to explain adhesion to atomically flat surfaces, PVC is sufficiently strongly adhesive to 2D crystal flake surfaces to allow pickup from SiO$_2$/Si substrates via surface contact alone. Results of the pickup test, whether pickup is possible or impossible, were plotted on a map of contact surface area ratio vs. contact edge length ratio, which allowed us to identify the conditions under which flakes can be picked up using PVC and to discuss the adhesion strengths of the surface and edge. This study provides a method for the evaluation of adhesion forces between polymers and 2D flakes and demonstrates that PVC is a useful polymer for deterministic transfer and versatile manipulation of 2D flakes.

INTRODUCTION

Research on 2D materials has been growing rapidly. One of the most fascinating aspects of 2D materials is that they can be assembled into vertical stacks, called van der Waals (vdW) heterostructures[1], without the restriction of lattice matching. The freedom of choice of material and stacking order means that we have infinite possibilities in designing vdW heterostructures. To explore the field of vdW heterostructures, techniques for stacking 2D materials are essential[2]. Various types of polymers have been used to facilitate the assembly of 2D materials. The first reported 2D material transfer technique used polymethyl methacrylate (PMMA)[3]: The 2D flakes were exfoliated on a PMMA layer and then transferred onto a target flake. This type of transfer technique, in which flake stacks are assembled from the bottom to the top, is called bottom-up transfer. Polymers can be used as a pickup medium for 2D flakes on SiO$_2$/Si substrates: 2D flakes are picked up by a polymer stamp one by one, and this method is called top-down transfer[4]. Moreover, polymer sheets are also utilized as supporting layers to make larger flakes by mechanical exfoliation[5]. Various types of polymers have been reported to be applicable for 2D material transfer, including polypropylene carbonate (PPC)[4,6,7], polydimethylsiloxane (PDMS)[8,9], PMMA[3,10], polycarbonates (PC)[11], Elvacite[12], polyvinyl alcohol (PVA)[13,14], nitrocellulose[15], polycaprolactone[16], paraffin[17], polyvinyl acetate[18], and nail polish[19]. Each polymer has different characteristics, and an appropriate polymer must be selected depending on the specific requirements of the situation. More recently, versatile manipulation—including sliding, folding, and peeling—of 2D flakes has been demonstrated using polyvinyl chloride (PVC)[20]. The key point of the manipulation was the strong adhesion of PVC, which enabled the control of the entire 2D flake only with a small part of the flake contacted by PVC.

In this study, we evaluated the adhesion of PVC to 2D flakes using a novel approach. In particular, we were able to distinguish the effects of the surface and edge of the 2D flakes on the pickup force. Although the anchoring effect is not significant for 2D surfaces, we show herein that PVC adheres to atomically flat 2D surfaces strong enough to pickup the flake via surface contact alone, without any contact between the edge of the flake and the PVC.

RESULTS AND DISCUSSION

Preparation of PVC/PDMS stamp

Before proceeding to the main experiments, we present some key details of the PVC stamp preparation (full details are provided in the Supplementary information). We prepared a PVC/PDMS stamp on a glass slide for 2D flake pickup[20]. Here, we used a triple PDMS dome to specifically localize the area of contact between the PVC stamp and 2D flake. First, a PDMS dome was prepared on a glass slide as follows. A section of a PDMS sheet was attached to a glass slide, and liquid PDMS was dropped on the sheet to form a PDMS dome. The PDMS droplet was solidified by heating on a hotplate. To ensure that the tip of the PDMS dome possessed high curvature (diameter, ~30 µm, Supplementary Fig. 1a, b), we added further PDMS droplets to the PDMS dome, ultimately preparing a triple PDMS dome (Fig. 1a). Next, we covered the PDMS dome with PVC film (Supplementary Fig. 2). The PVC film used was a commercially available PVC food wrap (Riken Technos) which included additives such as plasticizers. The degree of polymerization of the PVC was ~1000, and the thickness of the film was ~7 µm. Before use, the surface of the PVC/PDMS stamp was gently cleaned with isopropyl alcohol on a dustless wiper to remove contaminants. We confirmed that the transfer can be conducted using PVC films fabricated from conventional PVC powder and plasticizer instead of commercially available PVC food wraps. (see Supplementary Information).

Systematical analysis on the adhesion of PVC to 2D crystal flakes

PVC exhibits strong adhesion to 2D flakes as demonstrated by versatile 3D manipulation of 2D materials[20]. Notably, we observed that PVC adheres to the atomically flat surfaces of 2D crystal flakes, as we will describe in detail below. Several mechanisms account for the adhesion force between polymers and 2D flakes. One of these mechanisms is the anchoring effect. The anchoring effect

[1]Institute of Industrial Science, University of Tokyo, 4-6-1 Komaba, Meguro, Tokyo 153-8505, Japan. [2]Research Center for Functional Materials, National Institute for Materials Science, 1-1 Namiki, Tsukuba 305-0044, Japan. [3]International Center for Materials Nanoarchitectonics, National Institute for Materials Science, 1-1 Namiki, Tsukuba 305-0044, Japan. ✉email: monodera@iis.u-tokyo.ac.jp; tmachida@iis.u-tokyo.ac.jp

explains the mechanical aspect of adhesion. The adhesive (polymer) fits into the surface structure of an adherend, and adhesion is reinforced. Thus, adhesion is strong when the surface of the adherend is rough (having pits or cracks). Considering the atomically flat nature of the surface of 2D flakes, the anchoring effect is not involved in the adhesion process. However, flake edges are not flat on the nanometer scale and are hence more susceptible to adhesion to polymers via the anchoring effect (Fig. 1c). However, as we will show later in this paper, PVC adheres to both the edges and surfaces of flakes. To evaluate and understand the excellent adhesion of PVC, we employed a novel experimental approach. Our experiment and analysis were systematically designed to qualitatively characterize the adhesion force, while also enabling a semi-quantitative comparison between the surface and edge adhesions of 2D crystal flakes. The features of our method are as follows: (1) a 2D crystal flake is shaped into a circular form to minimize the effects of shape variation on the pickup behavior, (2) the effects of the surface and edge are distinguished by varying the contact position in a controlled manner, and (3) a plot of the contact surface area vs. contact edge

length for each contact position reveals the surface and edge contributions to the adhesion of the 2D crystal flake.

The nature of the adhesion between the polymer and 2D flakes depends on the shape and size of the 2D flakes. For quantitative and systematic evaluation of the polymer adhesion force, the size and shape of the flakes should be normalized. Therefore, we exfoliated hexagonal boron nitride (h-BN) grown at high pressure and high temperature[21] onto a SiO_2/Si substrate and shaped the flakes (~30 nm thick) into circles (Fig. 1b, radius ~12 μm) via CF_4 plasma etching. The resultant circular shapes are highly symmetrical and minimize shape-related adhesion bias effects. Using the circular h-BN flakes, we conducted pickup tests using PVC. Figure 1a, b show schematics of the stamping apparatus and circular h-BN pickup procedure using the PVC/PDMS stamp, respectively. 2D flakes on a SiO_2/Si substrate were picked up using the stamp. Flakes of h-BN exfoliated onto a SiO_2/Si substrate were placed on a stage controlled by the actuator with stepper motors. The PVC stamp on a glass slide was fixed on the upper stage, and the contact between the PVC stamp and the h-BN flakes was made by lifting the bottom stage. Then, the bottom SiO_2/Si substrate was
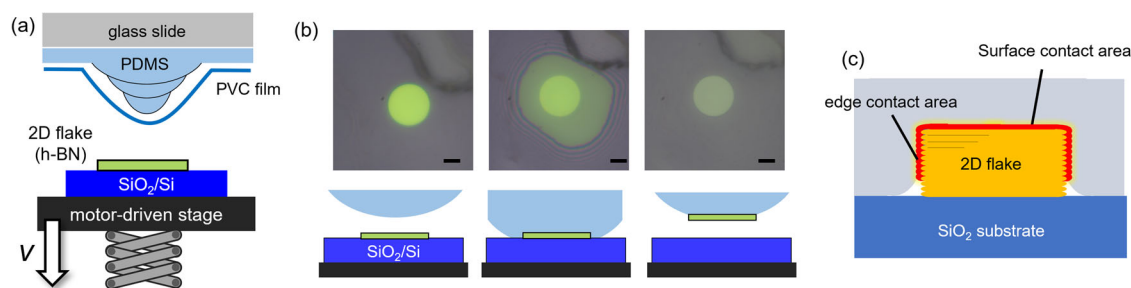

Fig. 1 Pickup of h-BN flakes using PVC/PDMS stamp. a Schematic of the stamping apparatus. The sample stage is controlled by an actuator with stepper motors, which enables precise control of the stage speed *v*. **b** Photographs and schematics of the pickup procedure. Scale bar: 10 μm. **c** Schematic showing the area on a 2D flake over which adhesion to the PVC stamp occurs (highlighted in red).
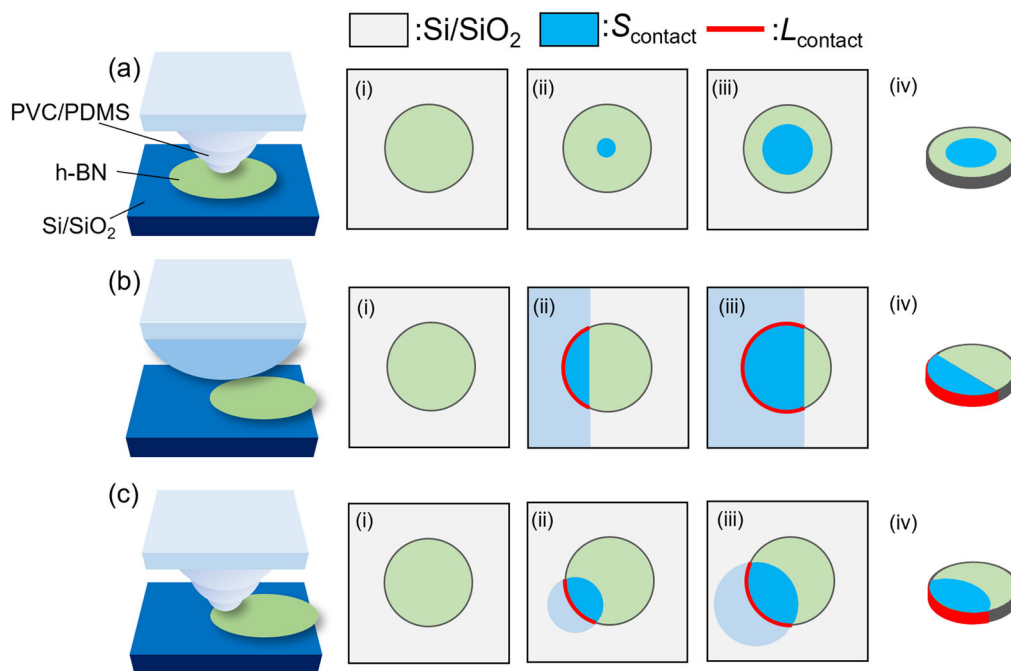

Fig. 2 Schematics of the pickup tests. a Pickup by surface contact alone using the PVC/triple PDMS dome. **b** Pickup by edge contact with minimal surface contact area using the PVC/semicylindrical PDMS, where the relationship between r_S and r_L is given by Eq. (1). **c** Pickup by edge and surface contact using the PVC/triple PDMS dome. The sky blue and red regions in (i–iv) indicate the areas of surface contact and edge contact between the PVC and h-BN, respectively.
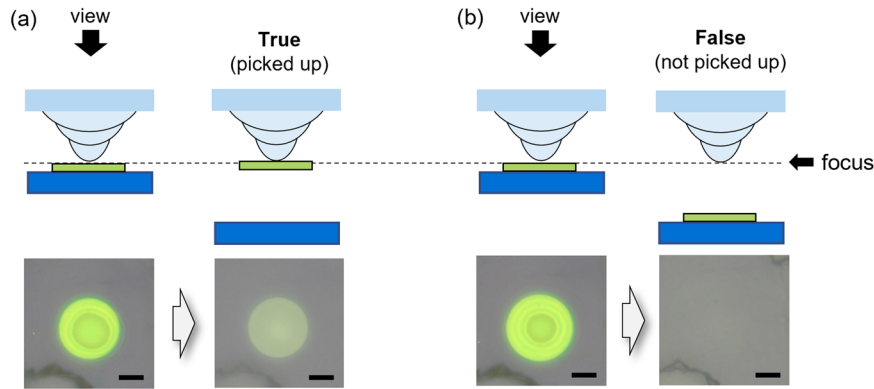
Fig. 3 Schematics and images of the pickup tests. Cases where h-BN is **a** picked up and **b** not picked up. The microscope was focused on the position indicated by the dashed line. Scale bar: 10 μm.
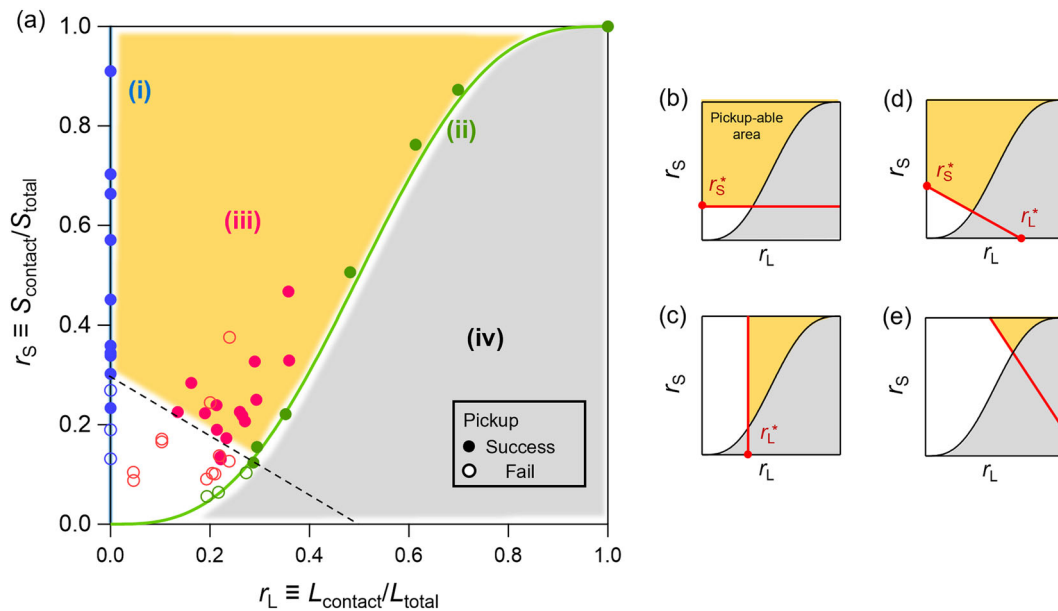

Fig. 4 Evaluation of surface and edge adhesion. a Plot of pickup test results versus relative contact surface area and relative contact edge length. Closed circles indicate successful pickups and open circles indicate unsuccessful pickups. The blue, green, and red colors correspond to the pickup by (i) surface contact alone, (ii) mainly-edge contact, and (iii) edge and surface contact, respectively (see discussion in the main text). The green line was calculated using Eq. (1). The yellow-shaded region is the region in which pickup occurs (the pickup region), and the white region is the region in which pickup is impossible. The gray-shaded region (iv) is the experimentally unfeasible region. **b**–**e** Schematics of the pickup regions: **b** surface-dominant adhesion, **c** edge-dominant adhesion, **d**, **e** both surface and edge adhesion. **d** is the case where 2D flakes can be picked up by surface contact alone, and **e** is the case where 2D flakes cannot be picked up by surface contact alone.

detached from the stamp by lowering the stage. The 2D flake was either picked up by the PVC stamp or remained on the SiO_2/Si substrate. Initial tests demonstrated that the stage speed v was an important parameter for successful flake pickup, and v was precisely controlled by the stepper motors (Fig. 1a). In Fig. 1b, we show photographs of the successful pickup of an h-BN flake using the stamp at $T = 70\,°C$. Whether a flake is picked up depends on the stage speed and temperature, as well as the area on the flake that comes into contact with the PVC stamp. In the subsequent PVC pickup tests, we fixed the stage speed v at 500 μm s^{-1} and the stage temperature T at 80 °C.

First, we focus on the adhesion between PVC and the surface of the h-BN flake. Figure 2a shows a schematic of the surface pickup test. To exclude edge effects, we ensured that contact between the PVC stamp and the h-BN surface occurred only at the center of the flake (sky blue region in Fig. 2a). Then, the PVC stamp was detached from the substrate by reversing the direction of motion

of the stage, i.e., by lowering the sample stage. At this point, the flake had been either picked up by the PVC stamp or had remained on the SiO_2/Si substrate, depending on the force between the PVC and flake surfaces (Fig. 3). Pickup occurred when the adhesion force between the PVC and the flake was larger than that between the flake and the SiO_2/Si substrate. We repeated this process, varying the contact area ratio $r_S \equiv S_{contact}/S_{total}$, where $S_{contact}$ is the surface area of the flake in contact with the stamp and S_{total} is the total surface area of the flake and recorded whether the flake was picked up (Supplementary Table 1). Pickup was successful when r_S was greater than 0.30. Because the adhesion force is assumed to be proportional to the contact area, this value can be regarded as the critical contact area ratio.

We next focus on the effect of the flake edge. To systematically discuss the edge effects and surface effects during pickup, we created a PVC/PDMS stamp based on a semicylindrical PDMS structure (Fig. 2b). This was prepared by placing PDMS liquid on a

PDMS sheet cut into a long rectangle (Supplementary Fig. 1c). Although some of the surfaces were also in contact with the stamp, the semicylindrical PDMS shape ensured that the contact surface area ratio r_S was minimized for the same contact edge length ratio $r_L \equiv L_{contact}/L_{total}$, where $L_{contact}$ is the length of the edge of the flake in contact with the stamp and L_{total} is the total edge length for the flake (mainly-edge pickup condition). The border of the contact region was initially set to the tangent of the circular h-BN flake and was moved such that it remained parallel to its original position (Fig. 2b). In this case, the relationship between r_S and r_L is given by an analytical formula:

$$r_S = r_L - \frac{\sin(2\pi r_L)}{2\pi}. \qquad (1)$$

(see Supplementary Fig. 3 and preceding discussion for the derivation of Eq. (1)). We repeated this procedure whilst varying r_L with r_S given by Eq. (1) (Supplementary Table 1). The pickup was observed to be successful when r_L was greater than 0.29.

Further, we conducted pickup tests under the intermediate conditions between the surface-only and mainly-edge pickup conditions discussed above. This part of the study uses the triple PDMS dome previously used for the surface-only pickup, and the contact region extends beyond the chord joining the points defining the extent of the edge contact (Fig. 2c). We repeated the pickup test whilst varying r_S and r_L, and the results are listed in Supplementary Table 1.

The results of the three types of pickup tests discussed so far (surface-only, mainly-edge, and combined edge and surface contacts) are plotted in Fig. 4a. On the vertical axis, $r = S_{contact}/S_{total}$ is plotted, and on the horizontal axis, $r_L = L_{contact}/L_{total}$. The closed circles indicate successful pickup, and the open circles indicate unsuccessful pickup. This graph is divided into four regions. Region (i) is in fact a line (blue) corresponding to the vertical axis $r_L = 0$, i.e., surface contact without edge contact (Fig. 2a). Pickup was successful when $r_S \gtrsim 0.30$ ($r_L = 0$), as discussed in the previous paragraph (Supplementary Table 1). PVC adheres to the flake surface even without any anchoring effect, which is in stark contrast to our observations when PC was used as the pickup material, as discussed later. Region (ii), which is a line given by Eq. (1) (green), corresponds to mainly-edge pickup with minimal surface contact, achieved using the semicylindrical PDMS structure (Fig. 2b). Along this line, pickup was successful when $r_L \gtrsim 0.29$ (r_S given by Eq. (1)). Region (iii) (red) corresponds to pickup attempts via contact with both the surface and edge using the triple PDMS dome (Fig. 2c). The data point at $(r_L, r_S) = (1, 1)$ on the plot corresponds to the case in which the entire flake is covered by the stamp. Region (iv) (gray) corresponds to the experimentally unfeasible region.

The yellow-shaded region corresponds to the region in which pickup is likely to occur (the pickup region). The boundary between successful and unsuccessful pickup is highlighted by the dashed line in Fig. 4a. The boundary line defines the critical condition for pickup, and this can be expressed as

$$\frac{r_S}{r_S^*} + \frac{r_L}{r_L^*} = 1, \qquad (2)$$

where r_S^* and r_L^* are the critical contact surface ratio and critical contact edge length ratio, respectively. In our experiment, $r_S^* = 0.30$ and $r_L^* = 0.50$. When surface adhesion is dominant, the boundary does not depend on r_L, and $r_S^* \ll r_L^*$ (Fig. 4b). In contrast, when edge adhesion is dominant, the boundary is independent of r_S, and $r_S^* \gg r_L^*$ (Fig. 4c). The intermediate of these extreme cases ($r_S^* \sim r_L^*$) is shown in Fig. 4d, e. Surface-only pickup is possible in Fig. 4d and impossible in Fig. 4e. Our experimental results resemble the plot in Fig. 4d.

In the preceding pickup tests, the speed of the stage v and its temperature T were fixed at $v = 500\ \mu m\ s^{-1}$ and $T = 80\,°C$. These values were selected based on another series of pickup tests using

v ($\mu m/s$)	T (°C) 33	40	50	60	70	80	90	100	110	120	130
900				▨	▨	▨	▨	▨	▨		
600				▨	▨	▨	▨	▨			
500				▨	▨	▨	▨	▨			
200				▨	▨	▨	▨				
100				▨	▨	▨	▨				
50				▨	▨	▨	▨				
20				▨	▨	▨					
10				▨	▨						
1				▨	▨						
0.5					▨						
0.2					▨						
0.1											
0.05											
0.01											

Fig. 5   Results of pickup tests conducted using various values of v and T. Yellow cells indicate successful pickups and light blue cells indicate unsuccessful pickups.

PVC/PDMS in which v and T were varied. In general, flakes are more likely to be picked up when the stage speed is higher, as has been reported for other polymers such as PDMS[8,22]. Similarly, the stage speed seems to enhance the adhesion force between the PVC surface and the flake. We conducted pickup tests with precise control of v using our motor-driven stage. Contact between the h-BN and PVC stamp was made at a stage speed of $10\ \mu m\ s^{-1}$ (fixed), and then the stage and the flake were detached at the speed of v. Starting from a small v, we repeated the contact–detach movements using the same flake and increasing v, recording whether the flake was picked up. Figure 5 lists the test results, with yellow cells indicating successful pickups and light blue cells indicating unsuccessful pickups. It should be noted that although the result is indicated as either yellow or light blue, the pickup probability gradually changed in the vicinity of the boundary of yellow and light blue. From this figure, we defined threshold stage speed v^* corresponding to the limiting value for flake pickup. v^* was minimized at $T \sim 70\,°C$. Considering that the stage speed compensates for the pickup force, the adhesion between the PVC and the flake is greatest at $T \sim 70\,°C$, which approximately corresponds to the glass transition temperature T_g of PVC.

We also conducted pickup tests using PC, which is a commonly used pickup polymer[11]. A thin PC film was placed on the triple PDMS dome on a glass slide, and we conducted pickup tests as in the case of PVC. The stage speed and temperature were fixed at $v = 500\ \mu m\ s^{-1}$ and $T = 110\,°C$. Supplementary Fig. 4 shows the results of the pickup test using PC, which resembles the schematic of Fig. 4e rather than Fig. 4d. In contrast to PVC, PC cannot pickup the flake via surface adhesion alone as far as we have optimized. This result suggests that the PC film cannot pickup the flake without the occurrence of an anchoring effect at the edge.

So far, we have shown that PVC is adhesive to both the surface and the edge of 2D flakes. This strong adhesion is highly useful for the fabrication of vdW heterostructures (Supplementary Fig. 5). Besides thick h-BN, monolayer graphene and monolayer MoS_2 can be picked up by PVC. Thus, this method is applicable to various 2D materials. Moreover, the flake can be released on a SiO_2/Si substrate at $T = 130\,°C$ without melting the PVC (Supplementary Fig. 6), that is, PVC can transfer 2D flakes without the need for immersion in a solvent. The surface of the transferred flakes can be easily cleaned by high-temperature annealing (Supplementary

Fig. 7). Additionally, once a structure has been fabricated, the PVC stamp can be reused until it is severely damaged. This reusability increases the pickup reproducibility because the polymer stamp conditions are preserved.

Finally, we discuss the possible mechanisms of adhesion. Although the anchoring effect is responsible for mechanical adhesion, many more existing adhesion mechanisms should be considered[23] (Supplementary Fig. 8). Considering the *h*-BN flake surface is atomically flat and inert, static electricity is the most probable mechanism accounting for the observed strong adhesion between the PVC stamp and the 2D crystal surface. Because PVC includes negatively polarized chloride atoms, an electrostatic potential will be generated at the PVC surface. The electrostatic force between atomically flat surfaces is significant when the distance between the two interfaces is small at the atomic level[24]. Close to the pickup temperature, PVC is sufficiently soft to be molded to fit the surface of the flake, and the distance between the two interfaces is minimized to maximize the electrostatic force. It would be highly interesting to investigate the correlation between the chloride atom content of PVC and its pickup behavior in a future experiment.

In conclusion, we demonstrated that PVC adheres strongly to 2D flakes. The adhesion was first examined by repeatedly making contact between PVC and a 2D flake and then detaching them, changing the detachment speed and stage temperature. We then investigated the ratios of the surface and edge adhesion contributions by localizing the PVC contact area within specific regions of the flake. Although the anchoring effect does not occur for an atomically flat surface, the adhesion of PVC to the 2D flake surface was sufficiently strong to allow the pickup of flakes when only surface contact, with no edge contact, occurred. In addition to the specific results on the effectiveness of PVC as a pickup material, our findings demonstrate a practical evaluation technique that can be applied to other polymers.

METHODS

Fabrication of PVC/PDMS stamp

To make PDMS domes, a PDMS elastomer kit (SYLGARD®184, Dow Corning) was used. A polymeric base and curing agent were mixed at a 10:1 (w/w) ratio. To eliminate air bubbles, the liquid mixture was placed under a vacuum in a desiccator for ~10 min. Next, a small piece ($4\,mm^2 \times 4\,mm^2$) was cut from a PDMS sheet (PF-X4- 17 mil., Gel-Pak) and placed on a glass slide. A droplet of the PDMS liquid mixture was placed on the piece of PDMS sheet using a toothpick and then cured at 130 °C for 5 min on a hotplate. The diameter of the dome was ~2 mm. Next, another PDMS droplet was placed on the first dome to make the second dome, which had a diameter of ~0.4 mm, and this was then cured at 130 °C for 5 min. Finally, a third droplet was placed on the second dome to form a third dome of ~30 μm in diameter using a gold wire designed for wire bonding (diameter, 25 μm), and this was cured at 130 °C for 5 min. (Supplementary Fig. S1a, b).

To create the semicylindrical PDMS structure, an elongated rectangle (4 mm × 10 mm) was cut from a PDMS sheet and placed on a glass slide. The PDMS mixture was placed on the PDMS rectangle and then cured at 130 °C for 5 min on a hotplate. Finally, the PDMS structure was cut into semicylindrical sections ($4\,mm^2 \times 4\,mm^2$) (Supplementary Fig. 1c).

We used a PVC-based food wrap (Riken Technos) for the PVC stamp. First, the PVC wrap was placed on a glass slide. Double-sided tape was attached to form a square frame surrounding a ~$5\,mm^2 \times 5\,mm^2$ area of the PVC sheet (Supplementary Fig. 2). Then, the frame was cut out using a rotary cutter and transferred onto the triple PDMS dome on the glass slide with the adhesive tape facing the glass slide. The PVC sheet was attached to a glass slide to obtain the PVC/PDMS stamp in its final usable format. The surface of the PVC/PDMS dome was wiped with isopropyl alcohol to eliminate contaminants and then blown with N_2 gas. This wiping process was necessary because it was observed that oily substances, probably the plasticizer contained in the PVC wrap, covered the surface of the PVC wrap.

REFERENCES

1. Geim, A. K. & Grigorieva, I. V. Van der Waals heterostructures. *Nature* **499**, 419–425 (2013).
2. Onodera, M., Masubuchi, S., Moriya, R. & Machida, T. Assembly of van der Waals heterostructures: exfoliation, searching, and stacking of 2D materials. *Jpn. J. Appl. Phys.* **59**, 010101 (2020).
3. Dean, C. R. et al. Boron nitride substrates for high-quality graphene electronics. *Nat. Nanotechnol.* **5**, 722–726 (2010).
4. Wang, L. et al. One-dimensional electrical contact to a two-dimensional material. *Science* **342**, 614–617 (2013).
5. Huang, Z. et al. Versatile construction of van der Waals heterostructures using a dual-function polymeric film. *Nat. Commun.* **11**, 1–10 (2020).
6. Kinoshita, K. et al. Dry release transfer of graphene and few-layer h-BN by utilizing thermoplasticity of polypropylene carbonate. *npj 2D Mater. Appl.* **3**, 22 (2019).
7. Onodera, M. et al. Electrical control of cyclotron resonance in dual-gated trilayer graphene. *Nano Lett.* **19**, 8097–8102 (2019).
8. Castellanos-Gomez, A. et al. Deterministic transfer of two-dimensional materials by all-dry viscoelastic stamping. *2D Mater.* **1**, 011002 (2014).
9. Ma, X. et al. Capillary-force-assisted clean-stamp transfer of two-dimensional materials. *Nano Lett.* **17**, 6961–6967 (2017).
10. Uwanno, T., Hattori, Y., Taniguchi, T., Watanabe, K. & Nagashio, K. Fully dry PMMA transfer of graphene on *h*-BN using a heating/cooling system. *2D Mater.* **2**, 041002 (2015).
11. Purdie, D. G. et al. Cleaning interfaces in layered materials heterostructures. *Nat. Commun.* **9**, 5387 (2018).
12. Masubuchi, S. et al. Autonomous robotic searching and assembly of two-dimensional crystals to build van der Waals superlattices. *Nat. Commun.* **9**, 1413 (2018).
13. Cao, Y. et al. Movable-type transfer and stacking of van der Waals hetero-structures for spintronics. *IEEE Access* **8**, 70488–70495 (2020).
14. Shivayogimath, A. et al. Do-it-yourself transfer of large-area graphene using an office laminator and water. *Chem. Mater.* **31**, 2328–2336 (2019).
15. Rebollo, I. G., Rodrigues-Machado, F. C., Wright, W., Melin, G. J. & Champagne, A. R. Thin-suspended 2D materials: facile, versatile, and deterministic transfer assembly. *2D Mater.* **8**, 035028 (2021).
16. Son, S. et al. Strongly adhesive dry transfer technique for van der Waals het-erostructure. *2D Mater.* **7**, 041005 (2020).
17. Leong, W. S. et al. Paraffin-enabled graphene transfer. *Nat. Commun.* **10**, 867 (2019).
18. Qian, Y. et al. Universal 2D material film transfer using a novel low molecular weight polyvinyl acetate. *Appl. Surf. Sci.* **534**, 147650 (2020).
19. Haley, K. L. et al. Heated assembly and transfer of van der Waals heterostructures with common nail polish. *Nanomanufacturing* **1**, 49–56 (2021).
20. Wakafuji, Y. et al. 3D manipulation of 2D materials using microdome polymer. *Nano Lett.* **20**, 2486–2492 (2020).
21. Taniguchi, T. & Watanabe, K. Synthesis of high-purity boron nitride single crystals under high pressure by using Ba–BN solvent. *J. Cryst. Growth* **303**, 525–529 (2007).
22. Tiwari, A. et al. The effect of surface roughness and viscoelasticity on rubber adhesion. *Soft Matter* **13**, 3602–3621 (2017).
23. Myshkin, N. & Kovalev, A. Adhesion and surface forces in polymer tribology—A review. *Friction* **6**, 143–155 (2018).
24. Maboudian, R. & Howe, R. T. Critical review: adhesion in surface micromechanical structures. *J. Vac. Sci. Technol. B* **15**, 1 (1998).

AUTHOR CONTRIBUTIONS

Y.W. and T.M. conceived and designed the experiments; Y.W. performed the experiments with the help of M.O., S.M., R.M., and Y.Z., K.W. and T.T. grew the h-BN crystals; M.O., Y.W., and T.M. wrote the manuscript using contributions from all authors.

COMPETING INTERESTS

The authors declare no competing interests.

ADDITIONAL INFORMATION

Supplementary information The online version contains supplementary material available at https://doi.org/10.1038/s41699-022-00323-7.

Correspondence and requests for materials should be addressed to Momoko Onodera or Tomoki Machida.

Reprints and permission information is available at http://www.nature.com/reprints

Publisher's note Springer Nature remains neutral with regard to jurisdictional claims in published maps and institutional affiliations.